In Silico Identification of Apple Genome-Encoded MicroRNA Target Binding Sites Potentially Targeting the ACLSV

Muhammad Aleem Ashraf [*,†] , Nimra Murtaza [†] , Judith K Brown , Naitong Yu [*]

Posted Date: 8 May 2023

doi: 10.20944/preprints202305.0517.v1

Keywords: trichovirus; in silico tools; apple chlorotic leaf spot virus; miRNA; RNA interference

Article

In Silico Identification of Apple Genome-Encoded MicroRNA Target Binding Sites Potentially Targeting the ACLSV

Muhammad Aleem Ashraf [1,2,*,†], Nimra Murtaza [2,†], Judith K. Brown [3] and Naitong Yu [1,*]

[1] Institute of Tropical Biosciences and Biotechnology, Chinese Academy of Tropical Agricultural Sciences, Haikou 571101, China
[2] Institute of Biological Sciences, Faculty of Natural and Applied Sciences, Khwaja Fareed University of Engineering and Information Technology, Rahim Yar Khan 64200, Pakistan; nimramurtaza196@gmail.com
[3] School of Plant Sciences, The University of Arizona, Tucson, AZ 85721, USA; jbrown@ag.arizona.edu
* Correspondence: ashraf.muhammad.aleem@gmail.com (M.A.A.); yunaitong@163.com (N.Y.)
† These authors contributed equally to this work.

Abstract: Apple chlorotic leaf spot virus (ACLSV) is a widespread, deleterious and the most damaging pathogen of fruit tree plants including domesticated apple (*Malus domestica*) —a great threat to apple production worldwide. The positive-sense single-stranded RNA genome of ACLSV (7.5 Kbp) encodes three proteins: RNA polymerase (Rep), movement protein (MP) and coat protein (CP). RNA interference (RNAi)-mediated antiviral innate immunity is a key sequence-specific biological phenomenon in eukaryotes to control plant viruses. The aim of this study was to analyze apple (*M.domestica*) locus-derived microRNAs (mdm-miRNAs) with predicted potential for targeting the ACLSV +ssRNA-encoded mRNAs, using 'four algorithms' approach. The ultimate goal in this research is to mobilize the in silico endogenous predicted mdm-miRNAs to trigger RNAi catalytic pathway experimentally and generate apple tree varieties for evaluating potential antiviral resistance monitoring capability and capacity for ACLSV. Experimentally validated mature apple (*M.domestica*, $2n = 2X = 34$) mdm-miRNAs ($n = 322$) were acquired from miRBase database and tested for alignment with the ACLSV genome. Of the 322 targeting mature locus-derived mdm-miRNAs investigated, nine apple mdm-miRNA homologs (mdm-miR395k, mdm-miR5225c and mdm-miR7121 (a, b, c, d, e, f, g, h) were predicted by all 'four algorithms'. Only fifty eight mdm-miRNAs were predicted consensus binding sites by union of consensus between two algorithms. The miRanda, RNA22, TAPIR algorithms predicted binding of mdm-miR395k at unique nucleotide position 4691, as the most effectively interacting mdm-miRNAs in targeting the ORF1 sequence. In order to validate target prediction accuracy, whether the apple mdm-miRNAs might bind predicted ACLSV mRNA target(s), we created an integrated Circos plot. Genome-wide in-silico-predicted miRNA-mediated target gene regulatory network validated interactions that warrant in vivo analysis. The current work provides valuable evidence and biological material for generating ACLSV-resistant apple varieties.

Keywords: *trichovirus*; in silico tools; *apple chlorotic leaf spot virus*; miRNA; RNA interference

1. Introduction

The cultivated Apple (*Malus domestica* Borkh) is an economically and culturally popular, most frequently produced fruit worldwide [1–3]. The first reference whole genome for domesticated apple ($2n = 2X = 34$) was released in 2010 [4]. *Apple chlorotic leaf spot virus* (ACLSV) is classified within the *Trichovirus* genus. ASLSV is an economically important, highly deleterious, graft-transmissible, latent pathogen that is distributed worldwide infecting cultivated, ornamental and wild fruit species plants including apple tree [5–9]. The genome of ACLSV (7474–7561 nucleotides) is a positive-sense single-

 doi:10.20944/preprints202305.0517.v1

stranded (+ssRNA) that comprises three ORFs. ORF1 encodes a large protein, replication-associated protein (Rep). Movement protein (MP) was coded by ORF2. ORF3 encodes a coat protein (CP) [10–12].

In plants, microRNAs (miRNAs) perform a crucial role in various biological processes including development, growth, response to environmental stresses and host-virus interaction by controlling gene expression and regulation. They are typically 20-24 nucleotides in length and can bind to complementary sequences in messenger RNAs (mRNAs), leading to their degradation or repression of translation [13,14]. Plant miRNAs are generated from miRNA precursors (termed pri-miRNAs). Dicer-like1 (GCL1), Ribonuclease (RNase) III enzyme is responsible for processing pri-miRNA transcripts into precursor miRNAs (pre-miRNAs). DCL cleaves pri-miRNA stem-loop, releasing a double-stranded RNA molecule that contains the miRNA sequence. Further, intermediate duplexes (miRNA/miRNA*) formation, stabilization, incorporation to the RNA induced silencing complex (RISC), which guide miRNA to target mRNA by base-pairing rule to lead for repression [15–18].

The widespread occurrence of microRNA-directed RNA silencing based on RNA interference (RNAi) is a conserved, stronger innate defense mechanism to control plant viruses. It involves gene regulation, host–virus interactions, and a strong inhibiter of virus replication [19–21]. The artificial microRNA (amiRNA)-based gene silencing impart resistance in plants against invading viruses. The amiRNA has been utilized successfully in economically important plants against rice stripe virus [22] and cucumber green mottle mosaic virus [23].

Apple tree has been investigated for potential diverse molecular mechanism to explore mature miRNAs which are natural source of immunity during biotic and abiotic stresses, and are important for growth and development [24–28]. The apple genome was mapped with experimentally verified 322 mature mdm-miRNAs that were available from miRBase [29]. The high-confidence mdm-miRNAs are hypothesized to have predicted binding sites in the ACLSV genome. The current study is based on predicting homologous amiRNAs for silencing of the ACLSV. The research work summarized key strategies for analyzing most effective target sites of apple locus-derived mdm-miRNAs and miRNA-mRNA target site interactions in the ACLSV genome. The study aims to elucidate the predicted apple locus-derived-mdm-miRNAs to induce resistance against ACLSV in the transgenic apple plants in future.

2. Materials and Methods

2.1. Apple Mature MicroRNAs and ACLSV Genomic Data Source

Recent studies indicated 322 mature apple (*Malus domestica*) miRNA sequences (mdm-miRNA156-mdm-miR11020) (Accession IDs: MIMAT0025867-MIMAT0043631) which were available in the miRBase database (version 22) (http://mirbase.org/) [29]. The mature sequences of apple mdm-miRNAs were acquired for analysis (Supplementary Table S1). The whole genome (7545 bases) of ACLSV (Isolate, SY03) (GenBank Accession number KU870525) was retrieved from the NCBI GenBank database [30].

2.2. Analysis of Multiple mdm-miRNA Target-Pairs in ACLSV Genome

A computational 'four algorithm' approach was implemented for effective binding prediction of mdm-miRNAs with the ACLSV genome using publicly available tools−miRanda, RNA22, TAPIR and psRNATarget which are most widely used in research (Table 1). Mature sequences of apple genome-encoded mdm-miRNAs and genomic transcript of the ACLSV (in FASTA format) were analyzed.

Preprints (www.preprints.org) | NOT PEER-REVIEWED | Posted: 8 May 2023 doi:10.20944/preprints202305.0517.v1

Table 1. Summary of *in silico* prediction tools used.

Algorithms	Parameter	Features	Availability
miRanda	Score threshold= 140, Free energy=−20 Kcal/mol, Gap open penalty=−9.0 0 Gap extend penalty=−4.0 0	Seed-based interaction, Target site accessibility, free energy of RNA-RNA duplex, conservation	http://www.microrna.org/ (accessed 26 January 2023)
RNA22	Folding energy=−15 Kcal/mol Number of paired-up bases= 12, Sensitivity (63%), Specificity (61%),	Non-seed based interaction, Site complementarit y, Target site multiplicity, Pattern recognition, Folding energy of heteroduplex	https://cm.jefferson.edu/rna22/Interactive/ (accessed on 22 October 2022)
TAPIR	Free energy=−20 Kcal/mol, Hit per target= 1	Seed paring, Free energy of duplex, Multiple target sites,	http://bibiserv.techfak.uni-bielefeld.de/rnahybrid (accessed on 9 November 2022)
psRNATarg et	Expectatio n Score= 6.5, HSP size= 19, Penalty for G:U pair= 0.5 Penalty for opening gap= 2	Multiplicity of target site, Translation inhibition, Target accessibility, Complementarity scoring	https://www.zhaolab.org/psRNATarget/analysis?functio n=2 (accessed on 9 November 2022)

2.3. miRanda

The miRanda algorithm involves several features such as sequence complementarity, seed-based interaction, miRNA-mRNA duplex dimerization and was released in 2003 [31]. Cross-species target conservation is a key feature for prediction. It has been widely used standard scanning computational algorithm for prediction miRNA binding sites in the corresponding target region based on thermodynamically free energy of duplexes [32]. The miRanda algorithm has been written in C programming language. Standard parameters were set for miRNA-target prediction (Table 1).

 doi:10.20944/preprints202305.0517.v1

2.4. RNA22

The RNA22 algorithm uses a pattern-recognition approach relied on non-seed based interactions of miRNA-mRNA pairs. A web-based server is used for prediction miRNA binding sites in the target sequence [33]. Highly sensitive and significant target patterns were predicted based on maximum folding energy (MFE) [34]. Default parameters were selected for prediction of multiple target sites (Table 1).

2.5. TAPIR

The TAPIR algorithm is a newly developed web server used to select highly specific miRNA-mRNA duplexes precisely. TAPIR is also named as Tapirhybrid. It has been widely used to identify seed-based miRNA-target binding sites based minimum free energy ratio in plants [35]. Target prediction was performed on standards parameters (Table 1).

2.6. psRNATarget

The psRNATarget algorithm is based on pattern of cleavage, high sensitivity, and diversity and uses complementarity scoring schema for prediction multiple binding sites of plant miRNAs in the target sequences using a web-based server [36,37]. The published 207 apple mdm-miRNAs were selected in the web server for analysis. Default standard parameters were selected for prediction of multiple target sites (Table 1).

2.7. Discovering Apple mdm-miRNA-Target Interactions

The apple mature mdm-miRNAs and target ORFs of ACLSV were plotted using CIRCOS algorithm [38].

2.8. RNAfold

The RNAfold algorithm is a web server implemented in ViennaRNA package [39]. It is used to construct the secondary structures of consensus mdm-miRNA precursors. Precursor sequences of apple mdm-MIRNAs were analyzed using default setting in the RNAfold web server.

2.9. RNAcofold

The RNAcofold algorithm is used to evaluate miRNA-mRNA interactions by estimating free energy (ΔG) of duplexes [40]. Consensus fasta sequences of mature apple mdm-miRNAs and target sequences of ACLSV were analyzed using default setting in the RNAcofold web server.

2.10. Statistical Analysis

The predicted miRNA datasets presented here were generated as graphical interpretations. The R-language (version 3.1.1) is widely used tool for biological data interpretation and visualization [41].

3. Results

3.1. Apple Genome-Encoded mdm-miRNAs Targeting ACLSV Genome

The in-silico approach to identify apple mdm-miRNAs with predicted potential for targeting the ACLSV +ssRNA-mRNA among the 322 apple genome-encoded mature mdm-miRNAs was investigated using a focused bioinformatic 'four algorithms' approach. The miRanda algorithm predicted binding of 37 mature apple mdm-miRNAs at 46 target sites in the ACLSV genome. RNA22 predicted 108 mdm-miRNAs targeting 161 genomic sites of ACLSV. The TAPIR algorithm identified 103 apple genome-encoded mdm-miRNA-target pairs. In contrast, highly significant 'cleavable targets' were identified by the psRNATarget algorithm: 109 mdm-miRNAs targeting at 166 genomic sites of ACLSV (Table S2-S3 and File S1).

Preprints (www.preprints.org) | NOT PEER-REVIEWED | Posted: 8 May 2023 doi:10.20944/preprints202305.0517.v1

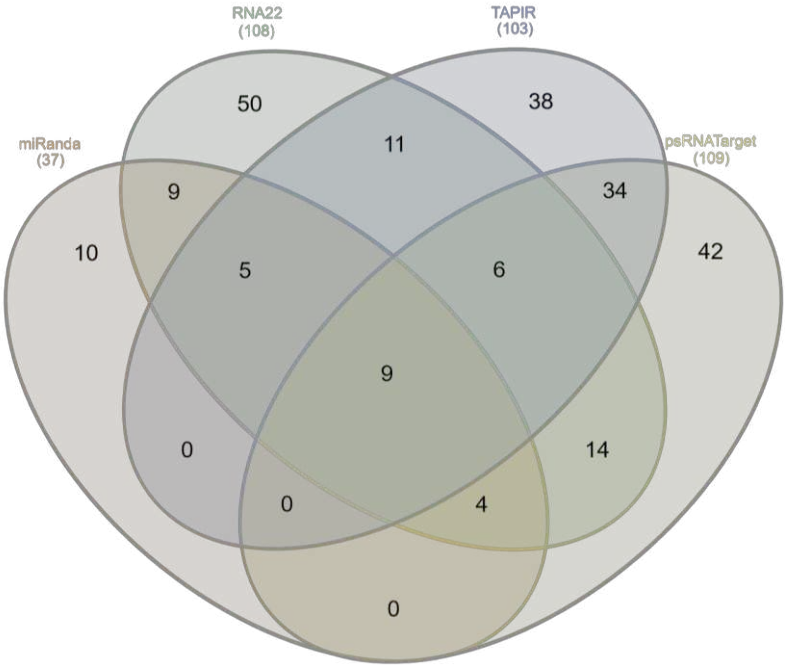

Figure 1. Venn diagram plot of apple genome-encoded mdm-miRNAs predicted for interacting with the ACLSV ssRNA genome. In this study, four algorithms (namely miRanda, RNA22, TAPIR, and psRNATarget) were selected for the identification of 'effective apple mdm-miRNA-binding sites' in the ACLSV genome**.** To the extent of degree of overlapping between in silico tools was determined at binding sites level. The intersection of four tools in this Venn plot concluded nine unique apple mdm-miRNAs.

3.2. Apple mdm-miRNAs Targeting ORF1 that Ecodes Replication-asscoiated Protein

The trichoviral ORF1 (140-5773) (5634 bases) encodes the replication associated polyprotein (Rep) containing RNA-dependent RNA polymerase (RdRp), which is essential for genome replication [42,43]. The miRanda algorithm predicted binding of thirty one apple mdm-miRNAs: mdm-miR159c (start site 4379), mdm-miR160 (a, b, c, d, e) (4197), mdm-miR169a (4217, 3355), mdm-miR169 (e, f) (1571), mdm-miR169 (g, h, i and j) (4217,3355), mdm-miR393 (g, h) (3091), mdm-miR395k (4691), mdm-miR3627d (2376), mdm-miR5225 (a, b) (182), mdm-miR5225c (4719), mdm-miR7121 (a, b, c, d, e, f, g and h) (149), mdm-miR10998 (3899) and mdm-miR11012 (a, b) (4585) (Figure 2A). RNA22 predicted eighty two apple mdm-miRNAs: mdm-miR160 (start site a, b, c, d, e,) (2133, 4424), mdm-miR166f (963, 4194), mdm-miR167a (975), mdm-miR167 (b, c, d, e ,f, g, h, i and j) (3231), mdm-miR168(a, b) (2504, 3030), mdm-miR169o (345), mdm-miR171f-3p (3230), mdm-miR171f-5p (5101), mdm-miR171o (836), mdm-miR171q (5101), mdm-miR172 (m, n) (3230), mdm-miR319 (a b-3p (5195), mdm-miR319c-5p (952, 1743, 3236), mdm-miR319h (952, 1743, 3236), mdm-miR393 (d, e, f, g, h) (3092), mdm-miR394 (a, b)(2587), mdm-miR395 (d-5p, g-5p, h, i-5p and j) (5181), mdm-miR395k (4691), mdm-miR395l (5592), mdm-miR408a (2376), mdm-miR477(a, b) (3659), mdm-miR482a-3p (2135), mdm-miR530 (a, b, c) (4683), mdm-miR535 (a, d) (1652), mdm-miR3627d (2376, 3541), mdm-miR5225 (a, b) (1364) mdm-miR5225c (1718), mdm-miR7121 (a, b, c) (153, 961, 2574), mdm-miR7121 (d, e, f, g, h) (2574, 4538), mdm-miR10978 (a, b)(1644), mdm-miR10979 (2150), mdm-miR10980 (a, b)(2630, 4198), mdm-miR10983 (5399), mdm-miR10984b-3p(2584), mdm-miR10993 (c, d, e, f) (972), mdm-miR10994-3p (2217), mdm-miR10995 (960, 4695), mdm-miR10996a (3100), mdm-miR11002 (a, b, c-3p) (558, 4139, 5331), mdm-miR11012(a, b) (4582) and mdm-miR11019 (964) (Figure 2B).

Preprints (www.preprints.org) | NOT PEER-REVIEWED | Posted: 8 May 2023 doi:10.20944/preprints202305.0517.v1

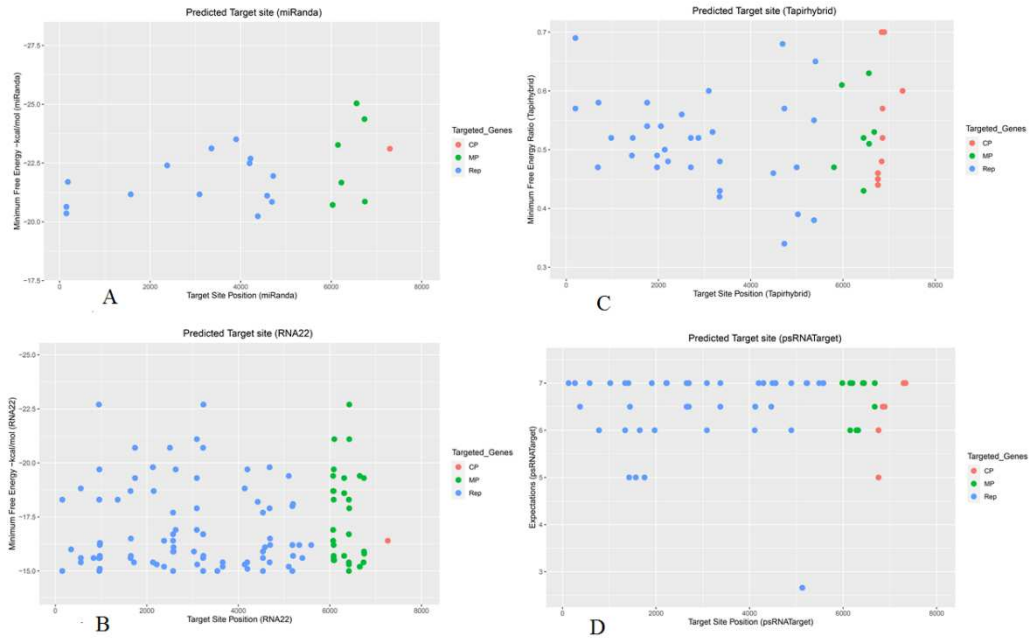

Figure 2. Mature apple mdm-miRNA-target prediction in the ACLSV genome was obtained using following in silico algorithms: (**A**) miRanda. (**B**) RNA22. (**C**) TAPIR or Tapirhybrid. (**D**) psRNATarget. Each colored dot shows a single binding site of predicted mdm-miRNA in the ACLSV genome. The ORFs in ACLSV genome is represented by a different color.

The TAPIR algorithm identified several mdm-miRNAs: mdm-miR167a (start site 976), mdm-miR168 (a, b) (2505), mdm-miR169 (k, l, m, n, o) (200), mdm-miR171 (m, n) (700), mdm-miR319 (b-5p, d, e, f) (5373), mdm-miR390 (a, b, c, d, e, f) (687), mdm-miR393 (d, e, f) (3091), mdm-miR394a (1426), mdm-miR394b (1970), mdm-miR395(a, b, c, d-3p, e, f, g-3p, h, and i-3p,) (1970), mdm-miR395k (4691), mdm-miR396 (a, c, d, e) (2702), mdm-miR397 (a, b) (3331), mdm-miR399 (e, f, g, h) (1443), mdm-miR403 (a, b) (2053), mdm-miR477a (2028), mdm-miR482a-3p (2136), mdm-miR482b (2207), mdm-miR530 (a, b, c) (4730), mdm-miR5225c (4490), mdm-miR7120 (a-3p, b-3p) (l2867), mdm-miR7121 (a, b, c, d, e, f, g and h) (1755), mdm-miR10981 (c, d) (5024), mdm-miR10983 (3324), mdm-miR10986 (5404), mdm-miR10989 (a, b, c, d, e) (3173) and mdm-miR10991(a, b, c, d, e) (4997) (Figure 2C). Several potential apple mature mdm-miRNAs were predicted by psRNATarget algorithm: mdm-miR156 (ad, ae) (2674), mdm-miR159 (a, b) (375), mdm-miR164 (b, c, d ,e, f) (2670), mdm-miR166(a, b, c, d, e, f, g, h and i) (781), mdm-miR169 (e, f) (2669), mdm-miR171o (581), mdm-miR172 (a,b ,c ,d ,e ,f ,g ,h ,I ,j ,k ,l ,m ,n, o) (5580), mdm-miR319 (a, b) (2232), mdm-miR394 (a, b) (1426, 4195), mdm-miR395 (a, b, c, d, e, f , g, h and i) (1970, 4121), mdm-miR396 (a, b, c, d, e, f, g) (2702, 3376), mdm-miR399 (e, f, g, h) (1443), mdm-miR408 (a) (2218, 1410), mdm-miR408 (b, c, d) (2668), mdm-miR482a-5p (4111), mdm-miR535 (a, d) (1652), mdm-miR858 (4465, 4296), mdm-miR2111 (a, b) (1021, 4893), mdm-miR5225 (a, b) (1340, 5233), mdm-miR5225c (266, 4490), mdm-miR7120 (a, b) (5128, 4556, 3088), mdm-miR7121(a, b, c, d, e, f, g and h) (1755), mdm-miR7123 (a, b) (1567), mdm-miR7125 (5489) and mdm-miR7126 (1910) (Figure 2D).

3.3. Apple mdm- miRNAs Targeting ORF2 that Encodes Movement Protein

The trichoviral ORF2 (5685-7067) (1382 nucleotides) encodes a multifunctional movement protein (MP) which is required for cell-to-cell movement for ACLSV [44–47]. The miRanda algorithm predicted several apple mdm-miRNAs to silence the movement protein by targeting ORF2: mdm-miR319d (start site 6744), mdm-miR828 (a, b) (6033), mdm-miR3627d (6736), mdm-miR5225 (a, b) (6226), mdm-miR10980 (a, b) (6561), mdm-miR11008 (6150) (Figure 2A).

RNA22 predicted binding of potential apple mdm-miRNAs to target ORF2: mdm-miR164 (a, b, c, d, e, f) (start site 6096), mdm-miR169 (e, f) (6750), mdm-miR171(a, b) (6071), mdm-miR171f-5p (6651), mdm-miR171 (j, k, l, p) (6071), mdm-miR171 (q) (6071, 5101), mdm-miR319d (6744), mdm-

Preprints (www.preprints.org) | NOT PEER-REVIEWED | Posted: 8 May 2023 doi:10.20944/preprints202305.0517.v1

miR393 (d, e, f)(6423), mdm-miR394 (a,b) (6746), mdm-miR399 (a, b, c, d, i, j) (6083), mdm-miR482a-5p (6657), mdm-miR530 (a, b, c) (6312), mdm-miR3627d(6736), mdm-miR7121 (a, b, c, d, e, f, g, h) (6415), and mdm-miR10981 (a, b) (6085) (Figure 2B). The TAPIR algorithm predicted eight mdm-miRNAs: mdm-miR169b (6678), mdm-miR396 (e, f) (6447), mdm-miR3627d (6567), mdm-miR7125 (5806), mdm-miR10980 (a, b) (6561), mdm-miR10994-3p (5976) (Figure 2C). Several potential apple mdm-miRNAs were predicted by the psRNATarget algorithms: mdm-miR169 (b, c, d) (6678), mdm-miR171o (5985), mdm-miR390 (a, b, c, d, e, f) (6321), mdm-miR393 (d, e, f) (6432), mdm-miR395 (a, b, c, d, e, f, g ,h, i) (6286), mdm-miR396 (f, g) (6447), mdm-miR397 (a, b) (6152), mdm-miR482b (6432) and mdm-miR5225c (6200) (Figure 2D).

3.4. Apple mdm- miRNAs Targeting ORF3 that Encodes Coat Protein

The trichoviral ORF3 (6751-7332 bp) (581 nucleotides) encodes a capsid protein (CP) for encapsidation of trichoviral ssRNA [48,49]. Only one mdm-miRNA (mdm-miR5225c) was detected at nucleotide position 7297 by the miRanda algorithm (Figure 2A). Two unique apple mdm-miRNAs were identified by RNA22: mdm-miR168 (a, b) (7265) (Figure 2B). Several potential apple mdm-miRNAs were predicted to target the ORF3 for silencing the coat protein by TAPIR algorithm: mdm-miR156 (p, q, r, s, x, y, z) (6758), mdm-miR156 (aa, ab, ac, ad, ae) (6758, 7293), mdm-miR397b (6839), mdm-miR398 (b, c) (6839), mdm-miR11001 (6858), mdm-miR11016 (6858) (Figure 2C). In addition, psRNATarget predicted nineteen mdm-miRNAs: mdm-miR156 (p, q, r, s) (6758), mdm-miR156 (ab, ac, ad, ae) (6758, 7293), mdm-miR166 (a, b, c, d, e, f, g, h, i) (7335), mdm-miR398a (6890) and mdm-miR858 (6846) (Figure 2D and Figure 3).

3.5. Evaluation of Common Apple MicroRNAs

On the basis of predicted apple genome-encoded mdm-miRNAs, nine miRNAs (mdm-miR5225c and mdm-miR7121 (a, b, c, d, e, f, g and h) were detected by union of consensus between 'all four algorithms' (Figure 1 and Figure 3).

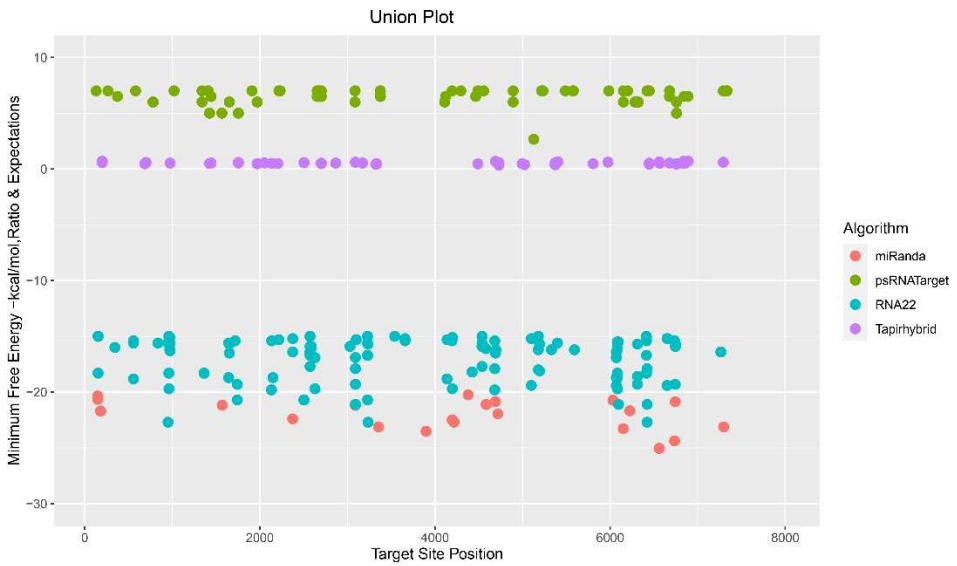

Figure 3. Union plot indicating the entire set of predicted apple mdm-miRNA-binding sites targeting ACLSV genome. This plot is created as a union by all tools.

3.6. Evaluation and Identification of Consensual Apple MicroRNAs for ACLSV Silencing

Of the 322 targeting mature apple tree mdm-miRNAs, 58 apple mdm-miRNAs (mdm-miR156 (start site o, p, q, r, ab, ac) at nucleotide (nt) position 6758, mdm-miR156 (ad, ae) at nt position 7293, mdm-miR167a at nt position 976, mdm-miR168 (a, b) at nt position 2505, mdm-miR169b at nt position 6678, mdm-miR319d at nt position 6744, mdm-miR393 (d, e, f, g, h) at nt positions 3092 and mdm-

Preprints (www.preprints.org) | NOT PEER-REVIEWED | Posted: 8 May 2023 doi:10.20944/preprints202305.0517.v1

miR393 (d, e, f) at nt positions, mdm-miR394a at nt position 1426, mdm-miR395 (a, b, c, d, e, f, g, h, i) at nt position 1970, mdm-miR395k at nt positions 4691, mdm-miR396 (a, c, d, e) at nt position 2702, mdm-miR396 (f, g) at nt positions 6447, mdm-miR399 (e, f, g, h) at nt position 1443, mdm-miR482a-3p at nt positions 2136, mdm-miR535(a, d) at nt position 1652, mdm-miR3627d at nt positions 2376 and 6736, mdm-miR5225c at nt positions 4490, mdm-miR7121 (a, b, c, d, e, f, g, h) at nt positions 153 and 1755, mdm-miR10980 (a, b) at nt positions 6561 and mdm-miR11012 (a, b) at nt positions 4585 were detected by consensus between two algorithms (Figure 4 and Table 2).

On the basis of identifying 58 consensus mdm-miRNAs, nine apple tree mdm-miRNAs, mdm-miR7121 (a, b, c, d, e, f, g, h) and mdm-miR395k were predicted top effective mdm-miRNAs for targeting the ACLSV genome (Figure 4).

Table 2. Target binding sites of consensus apple genome-encoded mdm-miRNAs, detected by union of consensus between two algorithms.

Apple miRNAs	Position miRanda	Position RNA22	Position TAPIR	Position psRNATarget	MFE * miRanda	MFE ** RNA22	MFE Ratio TAPIR	Expectation psRNATarget
mdm-miR156 (p, q, r, s)			6758	6758			0.44	6.00
mdm-miR156 (ab, ac)			6758	6758			0.46	5.00
mdm-156 (ad, ae)			7293	7293			0.60	7.00
mes-miR167a			975	976		−16.30	0.52	
mdm-miR168 (a, b)		2504	2505			−20.70	0.56	
mdm-miR169b			6678	6678			0.53	6.50
mdm-miR319d	6744	6744			−20.86	−18.10		
mdm-miR393 (d, e, f)		6423		6423		−19.30		7.00
mdm-miR393 (d, e, f)		3092	3091			−22.70	0.60	
mdm-miR393 (g, h)	3091	3092			−21.17	−21.11		
mdm-miR394 (a, b)			1426	1426			0.49	5.00
mdm-miR395 (a, b, c, d, e, f, g, h, i)			1970	1970			0.47	6.00
mdm-miR395k	4691	4691	4691		−20.85	−18.00	0.68	
mdm-miR396 (a, c, d, e)			2702	2702			0.52	6.50
mdm-miR396 (f, g)			6447	6447			0.43	7.00
mdm-399 (e, f, g, h)			1443	1443			0.52	6.50
mdm-482a-3p		2135	2136			−18.30	0.48	
mdm-482b			2207	2207			0.34	6.00
mdm-535a		1652		1652		−18.60		6.00
mdm-535b		1652		1652		−17.90		6.50
mdm-miR3627d	2376	2376			−22.40	−19.30		
mdm-miR3627d (1)	6736	6736			−24.37	−19.80		
mdm-5225c			4490	4490			0.46	7.00
mdm-7121 (a, b, c)	149	153	1755	1755	−20.63	−22.40	0.58	5.00
mdm-miR7121 (d, e, f, g, h)			1755	1755			0.58	5.00
mdm-miR10980 (a, b)	6561		6561		−25.04		0.63	
mdm-miR11012 (a, b)	4585	4582			−21.11	−18.82		

*MFE is an abbreviation of minimum free energy. MFE ** is the maximum folding energy.

Preprints (www.preprints.org) | NOT PEER-REVIEWED | Posted: 8 May 2023 doi:10.20944/preprints202305.0517.v1

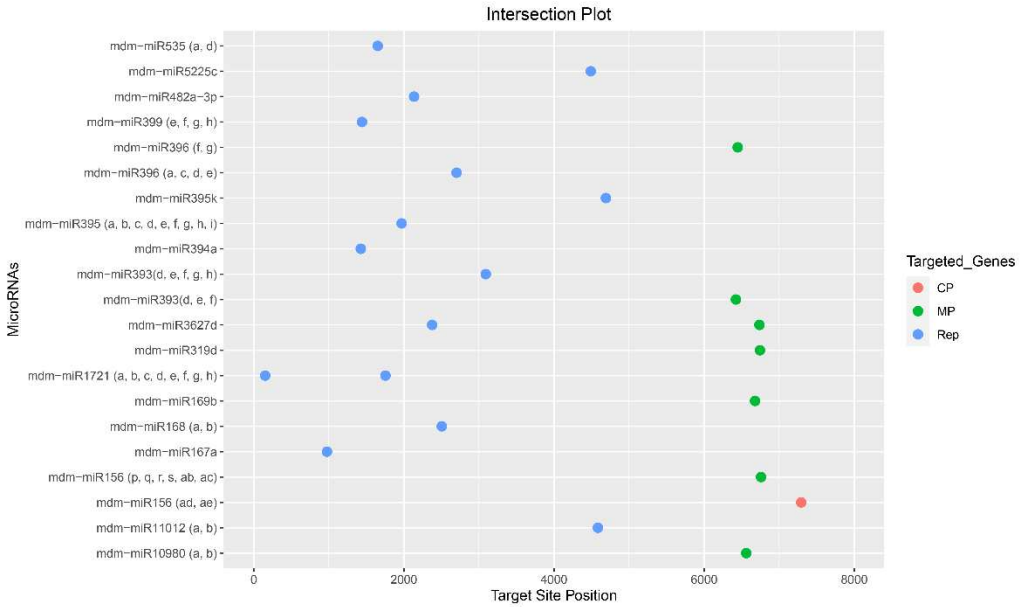

Figure 4. Intersection plot represent consensus apple mdm-miRNAs targeting ACLSV genome. Predicted mdm-miRNA-binding sites were selected by union of consensus between two algorithms.

3.7. Construction of Apple mdm-miRNAs Regulatory Network

Prediction and validation of host-virus interaction was visualized and created by a 'Circos map'. The predicted Circos plot shows a comprehensive global purview of the integrated apple mdm-miRNAs and corresponding target genes of the ACLSV genome (Figure 5).

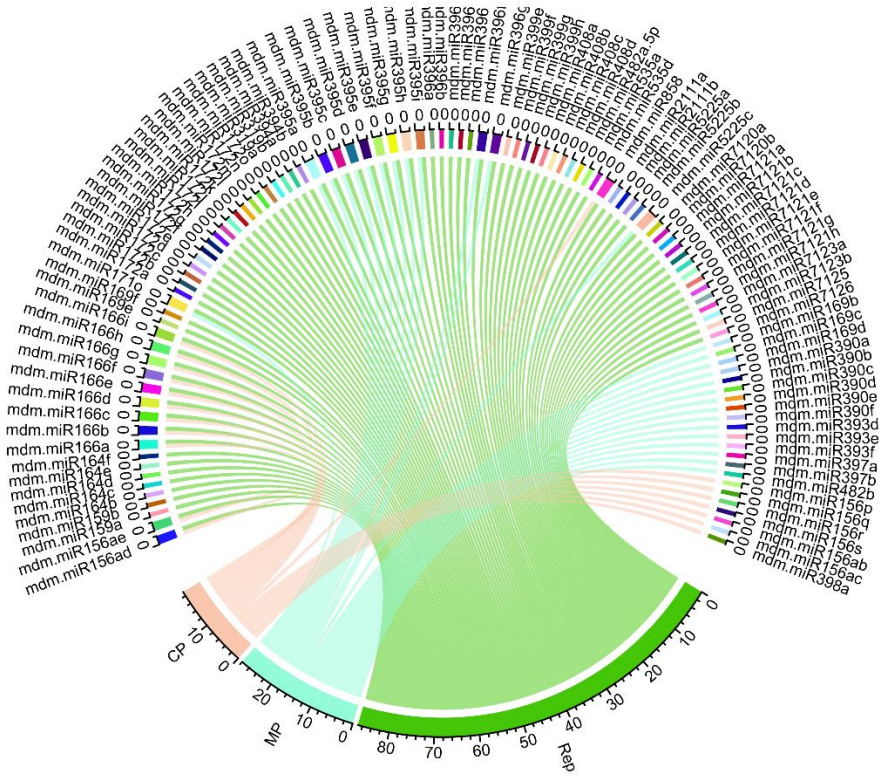

Figure 5. Integrated interaction map of apple genome-encoded mdm-miRNAs and ACLSV ORFs was represented. The ACLSV ORFs are shown as colored lines.

 doi:10.20944/preprints202305.0517.v1

3.8. Secondary Structures of the Consensual RNA

In silico identification, prediction and validation of the consensus apple genome-encoded mdm-miRNAs (mdm-MIR5225c, mdm-MIR395k and mdm-MIR7121 (a, b, c, d, e, f, g, h) was achieved by selecting and predicting their secondary structures using pre-miRNA sequences (Table 3).

Table 3. Characterization and salient features of consensus precursors of apple genome-encoded mdm-miRNAs evaluated in this study.

miRNA ID	Accession IDs	Length Precursor	MFE */Kcal/mol	AMFE **	MFEI ***	(G+C)%
mdm-MIR5225c	MI0023156	119 nt	−51.30	−43.10	−0.85	50.42
mdm-MIR395k	MI0035639	168 nt	−43.27	−25.75	−0.68	37.50
mdm-MIR7121a	MI0023144	132 nt	−49.40	−37.42	−0.79	46.97
mdm-MIR7121b	MI0023145	172 nt	−70.60	−41.04	−0.85	48.26
mdm-MIR7121c	MI0023146	135 nt	−71.30	−52.81	−1.09	48.15
mdm-MIR7121d	MI0023147	121 nt	−67.50	−55.78	−1.08	51.24
mdm-MIR7121e	MI0023148	121 nt	−67.50	−55.78	−1.08	51.24
mdm-MIR7121f	MI0023149	88 nt	−39.90	−45.34	−0.79	56.82
mdm-MIR7121g	MI0023150	100 nt	−45.80	−45.80	−0.89	51.00
mdm-MIR7121h	MI0023151	121 nt	−67.50	−55.78	−1.08	51.24

*MFE is the minimum free energy. **AMFE is an adjusted free energy. ***MFEI is free energy index.

3.9. Assessment of Free Energy

Evaluation and validation of consensus apple genome-encoded mdm-miRNAs were determined by assessment of their free energies (Δ*G)* of duplex bindings (Table 4).

Table 4. Free energy (Δ*G*) is generated after apple mdm-miRNA-mRNA duplex formation.

Apple mature miRNA ID	Accession ID	Mdm-miRNA-Target Sequence (5′–3′)	ΔG Duplex (Kcal/mol
mdm-miR5225c	MIMAT0026052	5′ UCUGUCGUGGGUGAGAUGGUGC 3′ 5′ GAAGCAGTGTACCCAAGACATA 3′	−15.90
mdm-miR395k	MIMAT0043586	5′ GUUUCCUCAAACACUUCAUU 3′ 5′ AGGCAGGAGTTTGAGGAAAC 3′	−18.30
mdm-miR7121a	MIMAT0026040	5′ UCCUCUUGGUGAUCGCCCUGU 3′ 5′ AAAGGGAGTTCATCGAGAGAA 3′	−22.10
mdm-miR7121b	MIMAT0026041	5′ UCCUCUUGGUGAUCGCCCUGU 3′ 5′ AAAGGGAGTTCATCGAGAGAA 3′	−22.10
mdm-miR7121c	MIMAT0026042	5′ UCCUCUUGGUGAUCGCCCUGU 3′ 5′ AAAGGGAGTTCATCGAGAGAA 3′	−22.10
mdm-miR7121d	MIMAT0026043	5′ UCCUCUUGGUGAUCGCCCUGC 3′ 5′ AAAGGGAGTTCATCGAGAGAA 3′	−22.10
mdm-miR7121e	MIMAT0026044	5′ UCCUCUUGGUGAUCGCCCUGC 3′ 5′ AAAGGGAGTTCATCGAGAGAA 3′	−22.10
mdm-miR7121f	MIMAT0026045	5′ UCCUCUUGGUGAUCGCCCUGC 3′ 5′ AAAGGGAGTTCATCGAGAGAA 3′	−22.10
mdm-miR7121g	MIMAT0026046	5′ UCCUCUUGGUGAUCGCCCUGC 3′ 5′ AAAGGGAGTTCATCGAGAGAA 3′	−22.10
mdm-miR7121h	MIMAT0026047	5′ UCCUCUUGGUGAUCGCCCUGC 3′ 5′ AAAGGGAGTTCATCGAGAGAA 3′	−22.10

4. Discussion

The ACLSV is a deleterious pathogen of fruit trees belonging to genus *trichovirus* that reduces plant vigor and yield causing viral infection in fruit trees produced in many countries during the last three decades. The discovery that amiRNA may act as a best strategy to control plant viruses has

 doi:10.20944/preprints202305.0517.v1

initiated extensive research in the field plant biotechnology [50]. Recent studies demonstrated expression of numerous endogenous plant miRNAs that may directly target RNA or DNA viruses using an in-silico approach—employing several computational algorithms [51–57]. Recent studies demonstrated expression of amiRNA-based constructs in economically important transgenic crops to eliminate plant viral load against RNA and DNA viruses [22,23,58–63]. Although several studies have already been performed on ACLSV pathogenesis, no research work was reported to enunciate the role of apple genome-encoded miRNA-mediated regulation targeting ACLSV viral replication. We highlight pivotal studies first time to test computationally the mature apple genome-encoded miRNAs for predicting effective miRNA-binding sites and to understand complex host-trichovirus specific interactions with the ORF1, ORF2 and ORF3 of ACLSV genome.

In silico algorithms are widely used to predict miRNA-binding sites in the target region to screen host-virus interaction [64]. The miRanda, RNA22 and TAPIR algorithms identified a consensual binding site of mdm-miR395k at nucleotide position 4691. The apple common madm-miR5225c and mdm-miR7121 (a, b, c, d, e, f, g, h) were predicted as the most potent miRNAs by all four algorithms (Figure 4 and Table 2). The TAPIR and psRNATarget algorithms were utilized to predict binding strength of madm-miR5225c and mdm-miR7121 (a, b, c, d, e, f, g, h) at consensus genomic positions 4490 and 1755, respectively.

For predicting miRNA-binding sites of the target sequence based on MFE which is also interpreted for evolutionary inferences [65]. The stability of miRNA-mRNA duplex is associated with the binding energy. Functional miRNA–target recognition depends upon site accessibility which is a key feature of in silico algorithms to assess the false-positive miRNA–target interaction. Validation of the miRNA–target interaction also depends upon MFE [66]. High probability of miRNA–target interaction was set on lower value of MFE [67]. High stability of miRNA-mRNA duplex is directly dependent on the stronger ability of binding affinity of miRNA to target mRNA [68,69]. Prediction, evaluation and validation of miRNA targeting patterns were based on base-pairing probability of mdm-miRNA seed regions with complementary high affinity binding sites in the ACLSV genome. The MFE of mdm-miR395k was calculated as −20.85 kcal/mol (miRanda), −18.00 kcal/mol (RNA22) (Table 2), and −18.30 kcal/mol (RNAcofold) (Tables 4), supporting prediction results with high stability of miRNA-mRNA duplex—representing 'true targets' [82,83].

Taken together with assessment of free energy is a standard feature of miRNA-target binding sites prediction which identified ten consensual potent apple miRNAs (Table 2, 3, 4). These predicted apple mdm-miRNAs have robust potential for RNAi-based gene silencing. Future work is focused on amiRNA-based constructs of ACLSV genome for transformation in apple plants.

Computational analysis have been implicated the apple consensus mdm-miR395k targeting ORF1 of ACLSV. The apple precursor mdm-MIR395k (NCBI Accession ID: MI0035639) was located on apple chromosome MDC003846.250 (genome context coordinates 8270 to 8437)[70]. Whereas in apple, Md-miR395 was demonstrated to target transcription factor *MdWRKY26* to regulate apple resistance to leaf spot disease [24]. The miR395 is involved in regulating carbohydrate accumulation gene (NADP-MDH) for flower development in tea-oil camellia [71]. Our studies show that apple genome-encoded miRNA pairs directly with specific locations on ACLSV +ssRNA-encoded mRNAs. In the current study, we demised a model to estimating the probability of prediction using different approaches to reduce false-positive results. These include at individual, union and intersection levels. Union approach is a highly sensitive for predicting candidate miRNAs based on combining more than one miRNA prediction tools. A lower level of prediction specificity was observed. While using intersection approach, which entirely based on prediction specificity suing more than two prediction tools with decrease in sensitivity of the predicted data [72]. Our reliable target prediction results demonstrated that in silico strategy concluded high efficiency of predicted data at individual, union and intersection levels with best target binding sites of apple mdm-miRNAs under study (Figure 1, 2, 3, 4 and Table 2).

While existing literature has mostly focused on full-length genome sequencing of ACLSV, here we identify apple genome-encoded miRNAs that bind directly to several consensuses genomic regions of ACLSV. In addition, there is no previous report that showed that apple tree mdm-miRNAs

bind to ACLSV predicting diverse, functionally related, host-miRNA-virus-mRNA interactions. While interactions between apple genome-encoded mdm-miRNAs and ACLSV were evaluated in this study, the probability of the apple mdm-miRNAs to bind ACLSV in vitro is needed to explore. While more studies need to be performed to fully comprehend the mechanism of host-virus interaction on the ACLSV genome at experimental level. This study deepens our understanding of ACLSV biology and validation of predicted miRNAs to develop resistant apple varieties. Further experiments are needed to determine binding strength of predicted mdm-miRNAs in transgenic apple plants in future.

Supplementary Materials: The following supporting information can be downloaded at the website of this paper posted on Preprints.org., Table S1: Apple tree mature mdm-miRNAs; Table S2: Identification apple mdm-miRNA-binding sites using multiple algorithms; Table S3: Gene wise prediction of mdm-miRNA-binding sites; File S1: Prediction results by different computational tools.

Author Contributions: M.A.A., J.K.B. and N.Y. conceived the original idea of the work. All the authors performed, analyzed, and interpreted the in silico data. All authors have read and agreed to the published version of the manuscript.

Funding: This research was funded by Hainan Provincial Natural Science Foundation (321RC640), and National Key R&D Program of China (2019YFD1000500). The research work was completed under a MoU among three institutes mentioned.

Institutional Review Board Statement: Not applicable.

Informed Consent Statement: Not applicable.

Data Availability Statement: Not applicable.

Conflicts of Interest: The authors declare no conflict of interest.

References

1. Na, W.; Wolf, J.; Zhang, F.-s. Towards sustainable intensification of apple production in China—Yield gaps and nutrient use efficiency in apple farming systems. *Journal of Integrative Agriculture* **2016**, *15*, 716-725.
2. Shah, Z.A.; Dar, M.A.; Dar, E.A.; Obianefo, C.A.; Bhat, A.H.; Ali, M.T.; El-Sharnouby, M.; Shukry, M.; Kesba, H.; Sayed, S. Sustainable Fruit Growing: An Analysis of Differences in Apple Productivity in the Indian State of Jammu and Kashmir. *Sustainability* **2022**, *14*, 14544.
3. Chen, Z.; Yu, L.; Liu, W.; Zhang, J.; Wang, N.; Chen, X. Research progress of fruit color development in apple (Malus domestica Borkh.). *Plant Physiology and Biochemistry* **2021**, *162*, 267-279.
4. Velasco, R.; Zharkikh, A.; Affourtit, J.; Dhingra, A.; Cestaro, A.; Kalyanaraman, A.; Fontana, P.; Bhatnagar, S.K.; Troggio, M.; Pruss, D. The genome of the domesticated apple (Malus× domestica Borkh.). *Nature genetics* **2010**, *42*, 833-839.
5. Martelli, G.; Candresse, T.; Namba, S. Trichovirus, a new genus of plant viruses. **1994**.
6. Rwahnih, M.A.; Turturo, C.; Minafra, A.; Saldarelli, P.; Myrta, A.; Pallás, V.; Savino, V. Molecular variability of apple chlorotic leaf spot virusin different hosts and geographical regions. *Journal of Plant Pathology* **2004**, 117-122.
7. Abtahi, F.; Shams-Bakhsh, M.; Safaie, N.; Azizi, A.; Autonell, C.R.; Ratti, C. Incidence and genetic diversity of apple chlorotic leaf spot virus in Iran. *Journal of Plant Pathology* **2019**, *101*, 513-519.
8. Katsiani, A.; Maliogka, V.; Candresse, T.; Katis, N. Host-range studies, genetic diversity and evolutionary relationships of ACLSV isolates from ornamental, wild and cultivated R osaceous species. *Plant pathology* **2014**, *63*, 63-71.
9. Yaegashi, H.; Yoshikawa, N.; Candresse, T. Apple chlorotic leaf spot virus in pome fruits. *Virus and Virus-Like Diseases of Pome and Stone Fruits; Hadidi, A., Barba, M., Candresse, T., Jelkmann, W., Eds* **2011**, 17-21.
10. Guo, W.; Zheng, W.; Wang, M.; Li, X.; Ma, Y.; Dai, H. Genome sequences of three apple chlorotic leaf spot virus isolates from hawthorns in China. *PLoS One* **2016**, *11*, e0161099.
11. Canales, C.; Morán, F.; Olmos, A.; Ruiz-García, A.B. First detection and molecular characterization of Apple stem grooving virus, apple chlorotic leaf spot virus, and apple hammerhead viroid in loquat in Spain. *Plants* **2021**, *10*, 2293.
12. Dhir, S.; Zaidi, A.A.; Hallan, V. M olecular C haracterization and R ecombination A nalysis of the C omplete G enome of A pple C hlorotic L eaf S pot V irus. *Journal of Phytopathology* **2013**, *161*, 704-712.

13. Reinhart, B.J.; Weinstein, E.G.; Rhoades, M.W.; Bartel, B.; Bartel, D.P. MicroRNAs in plants. *Genes & development* **2002**, *16*, 1616-1626.
14. Liu, W.-w.; Meng, J.; Cui, J.; Luan, Y.-s. Characterization and function of microRNA∗ s in plants. *Frontiers in plant science* **2017**, *8*, 2200.
15. Kim, Y.J.; Zheng, B.; Yu, Y.; Won, S.Y.; Mo, B.; Chen, X. The role of Mediator in small and long noncoding RNA production in Arabidopsis thaliana. *The EMBO journal* **2011**, *30*, 814-822.
16. Fang, X.; Cui, Y.; Li, Y.; Qi, Y. Transcription and processing of primary microRNAs are coupled by Elongator complex in Arabidopsis. *Nature Plants* **2015**, *1*, 1-9.
17. Fang, Y.; Spector, D.L. Identification of nuclear dicing bodies containing proteins for microRNA biogenesis in living Arabidopsis plants. *Current Biology* **2007**, *17*, 818-823.
18. Manavella, P.A.; Koenig, D.; Weigel, D. Plant secondary siRNA production determined by microRNA-duplex structure. *Proceedings of the National Academy of Sciences* **2012**, *109*, 2461-2466.
19. Trobaugh, D.W.; Klimstra, W.B. MicroRNA regulation of RNA virus replication and pathogenesis. *Trends in molecular medicine* **2017**, *23*, 80-93.
20. Deng, Z.; Ma, L.; Zhang, P.; Zhu, H. Small RNAs Participate in Plant–Virus Interaction and Their Application in Plant Viral Defense. *International Journal of Molecular Sciences* **2022**, *23*, 696.
21. Mengistu, A.A.; Tenkegna, T.A. The role of miRNA in plant–virus interaction: a review. *Molecular Biology Reports* **2021**, *48*, 2853-2861.
22. Zhou, L.; Yuan, Q.; Ai, X.; Chen, J.; Lu, Y.; Yan, F. Transgenic Rice Plants Expressing Artificial miRNA Targeting the Rice Stripe Virus MP Gene Are Highly Resistant to the Virus. *Biology* **2022**, *11*, 332.
23. Miao, S.; Liang, C.; Li, J.; Baker, B.; Luo, L. Polycistronic artificial microRNA-mediated resistance to cucumber green mottle mosaic virus in cucumber. *International journal of molecular sciences* **2021**, *22*, 12237.
24. Zhang, Q.; Li, Y.; Zhang, Y.; Wu, C.; Wang, S.; Hao, L.; Wang, S.; Li, T. Md-miR156ab and Md-miR395 target WRKY transcription factors to influence apple resistance to leaf spot disease. *Frontiers in Plant Science* **2017**, *8*, 526.
25. Qu, D.; Yan, F.; Meng, R.; Jiang, X.; Yang, H.; Gao, Z.; Dong, Y.; Yang, Y.; Zhao, Z. Identification of microRNAs and their targets associated with fruit-bagging and subsequent sunlight re-exposure in the "Granny Smith" apple exocarp using high-throughput sequencing. *Frontiers in plant science* **2016**, *7*, 27.
26. Niu, C.; Li, H.; Jiang, L.; Yan, M.; Li, C.; Geng, D.; Xie, Y.; Yan, Y.; Shen, X.; Chen, P. Genome-wide identification of drought-responsive microRNAs in two sets of Malus from interspecific hybrid progenies. *Horticulture research* **2019**, *6*.
27. Wang, Y.; Feng, C.; Zhai, Z.; Peng, X.; Wang, Y.; Sun, Y.; Li, J.; Shen, X.; Xiao, Y.; Zhu, S. The apple microR171i-SCARECROW-LIKE PROTEINS26. 1 module enhances drought stress tolerance by integrating ascorbic acid metabolism. *Plant physiology* **2020**, *184*, 194-211.
28. Tahir, M.M.; Li, S.; Liu, Z.; Fan, L.; Tang, T.; Zhang, X.; Mao, J.; Li, K.; Khan, A.; Shao, Y. Different miRNAs and hormones are involved in PEG-induced inhibition of adventitious root formation in apple. *Scientia Horticulturae* **2022**, *303*, 111206.
29. Kozomara, A.; Birgaoanu, M.; Griffiths-Jones, S. miRBase: from microRNA sequences to function. *Nucleic acids research* **2019**, *47*, D155-D162.
30. Sayers, E.W.; Beck, J.; Bolton, E.E.; Bourexis, D.; Brister, J.R.; Canese, K.; Comeau, D.C.; Funk, K.; Kim, S.; Klimke, W. Database resources of the national center for biotechnology information. *Nucleic acids research* **2021**, *49*, D10.
31. Enright, A.; John, B.; Gaul, U.; Tuschl, T.; Sander, C.; Marks, D. MicroRNA targets in Drosophila. *Genome biology* **2003**, *4*, 1-27.
32. John, B.; Enright, A.J.; Aravin, A.; Tuschl, T.; Sander, C.; Marks, D.S. Human microRNA targets. *PLoS biology* **2004**, *2*, e363.
33. Miranda, K.C.; Huynh, T.; Tay, Y.; Ang, Y.-S.; Tam, W.-L.; Thomson, A.M.; Lim, B.; Rigoutsos, I. A pattern-based method for the identification of MicroRNA binding sites and their corresponding heteroduplexes. *Cell* **2006**, *126*, 1203-1217.
34. Loher, P.; Rigoutsos, I. Interactive exploration of RNA22 microRNA target predictions. *Bioinformatics* **2012**, *28*, 3322-3323.
35. Bonnet, E.; He, Y.; Billiau, K.; Van de Peer, Y. TAPIR, a web server for the prediction of plant microRNA targets, including target mimics. *Bioinformatics* **2010**, *26*, 1566-1568.
36. Dai, X.; Zhao, P.X. psRNATarget: a plant small RNA target analysis server. *Nucleic acids research* **2011**, *39*, W155-W159.
37. Dai, X.; Zhuang, Z.; Zhao, P.X. psRNATarget: a plant small RNA target analysis server (2017 release). *Nucleic acids research* **2018**, *46*, W49-W54.

38. Krzywinski, M.; Schein, J.; Birol, I.; Connors, J.; Gascoyne, R.; Horsman, D.; Jones, S.J.; Marra, M.A. Circos: an information aesthetic for comparative genomics. *Genome research* **2009**, *19*, 1639-1645.
39. Lorenz, R.; Bernhart, S.; Siederdissen, C.; Tafer, H.; Flamm, C.; Stadler, P.; Hofacker, I. ViennaRNA package 2.0. algorithms for molecular biology. *vol* **2013**, *6*, 26-26.
40. Bernhart, S.H.; Tafer, H.; Mückstein, U.; Flamm, C.; Stadler, P.F.; Hofacker, I.L. Partition function and base pairing probabilities of RNA heterodimers. *Algorithms for Molecular Biology* **2006**, *1*, 1-10.
41. Gandrud, C. *Reproducible research with R and RStudio*; Chapman and Hall/CRC: 2018.
42. German, S.; Candresse, T.; Lanneau, M.; Huet, J.; Pernollet, J.; Dunez, J. Nucleotide sequence and genomic organization of apple chlorotic leaf spot closterovirus. *Virology* **1990**, *179*, 104-112.
43. Sato, K.; Yoshikawa, N.; Takahashi, T. Complete nucleotide sequence of the genome of an apple isolate of apple chlorotic leaf spot virus. *Journal of General Virology* **1993**, *74*, 1927-1931.
44. Singh, R.M.; Singh, D.; Hallan, V. Movement protein of Apple chlorotic leaf spot virus is genetically unstable and negatively regulated by Ribonuclease E in E. coli. *Scientific Reports* **2017**, *7*, 2133.
45. Satoh, H.; Matsuda, H.; Kawamura, T.; Isogai, M.; Yoshikawa, N.; Takahashi, T. Intracellular distribution, cell-to-cell trafficking and tubule-inducing activity of the 50 kDa movement protein of Apple chlorotic leaf spot virus fused to green fluorescent protein. *Journal of General Virology* **2000**, *81*, 2085-2093.
46. Yaegashi, H.; Takahashi, T.; Isogai, M.; Kobori, T.; Ohki, S.; Yoshikawa, N. Apple chlorotic leaf spot virus 50 kDa movement protein acts as a suppressor of systemic silencing without interfering with local silencing in Nicotiana benthamiana. *Journal of general virology* **2007**, *88*, 316-324.
47. Isogai, M.; Yoshikawa, N. Mapping the RNA-binding domain on the Apple chlorotic leaf spot virus movement protein. *Journal of general virology* **2005**, *86*, 225-229.
48. Yaegashi, H.; Isogai, M.; Tajima, H.; Sano, T.; Yoshikawa, N. Combinations of two amino acids (Ala40 and Phe75 or Ser40 and Tyr75) in the coat protein of apple chlorotic leaf spot virus are crucial for infectivity. *Journal of General Virology* **2007**, *88*, 2611-2618.
49. Mazeikiene, I.; Siksnianiene, J.B.; Gelvonauskiene, D.; Bendokas, V.; Stanys, V. Prevalence and molecular variability of Apple chlorotic leaf spot virus capsid protein genes in Lithuania. *Journal of Plant Diseases and Protection* **2018**, *125*, 389-396.
50. Niu, Q.-W.; Lin, S.-S.; Reyes, J.L.; Chen, K.-C.; Wu, H.-W.; Yeh, S.-D.; Chua, N.-H. Expression of artificial microRNAs in transgenic Arabidopsis thaliana confers virus resistance. *Nature biotechnology* **2006**, *24*, 1420-1428.
51. Ashraf, M.A.; Ali, B.; Brown, J.K.; Shahid, I.; Yu, N. In Silico Identification of Cassava Genome-Encoded MicroRNAs with Predicted Potential for Targeting the ICMV-Kerala Begomoviral Pathogen of Cassava. *Viruses* **2023**, *15*, 486.
52. Mohamed, N.A.; Ngah, N.M.F.N.C.; Abas, A.; Talip, N.; Sarian, M.N.; Hamezah, H.S.; Harun, S.; Bunawan, H. Candidate miRNAs from Oryza sativa for Silencing the Rice Tungro Viruses. *Agriculture* **2023**, *13*, 651.
53. Ashraf, M.A.; Tariq, H.K.; Hu, X.-W.; Khan, J.; Zou, Z. Computational Biology and Machine Learning Approaches Identify Rubber Tree (Hevea brasiliensis Muell. Arg.) Genome Encoded MicroRNAs Targeting Rubber Tree Virus 1. *Applied Sciences* **2022**, *12*, 12908.
54. Ashraf, M.A.; Feng, X.; Hu, X.; Ashraf, F.; Shen, L.; Iqbal, M.S.; Zhang, S. In silico identification of sugarcane (Saccharum officinarum L.) genome encoded microRNAs targeting sugarcane bacilliform virus. *PloS one* **2022**, *17*, e0261807.
55. Ashraf, M.A.; Ashraf, F.; Feng, X.; Hu, X.; Shen, L.; Khan, J.; Zhang, S. Potential targets for evaluation of sugarcane yellow leaf virus resistance in sugarcane cultivars: in silico sugarcane miRNA and target network prediction. *Biotechnology & Biotechnological Equipment* **2021**, *35*, 1980-1991.
56. Ashraf, F.; Ashraf, M.A.; Hu, X.; Zhang, S. A novel computational approach to the silencing of Sugarcane Bacilliform Guadeloupe A Virus determines potential host-derived MicroRNAs in sugarcane (Saccharum officinarum L.). *PeerJ* **2020**, *8*, e8359.
57. Gaafar, Y.Z.A.; Ziebell, H. Novel targets for engineering Physostegia chlorotic mottle and tomato brown rugose fruit virus-resistant tomatoes: in silico prediction of tomato microRNA targets. *PeerJ* **2020**, *8*, e10096.
58. Petchthai, U.; Yee, C.S.L.; Wong, S.-M. Resistance to CymMV and ORSV in artificial microRNA transgenic Nicotiana benthamiana plants. *Scientific reports* **2018**, *8*, 1-8.
59. Zhang, D.; Zhang, N.; Shen, W.; Li, J.-F. Engineered artificial microRNA precursors facilitate cloning and gene silencing in arabidopsis and rice. *International Journal of Molecular Sciences* **2019**, *20*, 5620.
60. Zhang, N.; Zhang, D.; Chen, S.L.; Gong, B.-Q.; Guo, Y.; Xu, L.; Zhang, X.-N.; Li, J.-F. Engineering artificial microRNAs for multiplex gene silencing and simplified transgenic screen. *Plant physiology* **2018**, *178*, 989-1001.

61. Yasir, M.; Motawaa, M.; Wang, Q.; Zhang, X.; Khalid, A.; Cai, X.; Li, F. Simple webserver-facilitated method to design and synthesize artificial miRNA gene and its application in engineering viral resistance. *Plants* **2022**, *11*, 2125.
62. Ali, I.; Amin, I.; Briddon, R.W.; Mansoor, S. Artificial microRNA-mediated resistance against the monopartite begomovirus Cotton leaf curl Burewala virus. *Virology journal* **2013**, *10*, 1-8.
63. Duan, C.-G.; Wang, C.-H.; Fang, R.-X.; Guo, H.-S. Artificial microRNAs highly accessible to targets confer efficient virus resistance in plants. *Journal of virology* **2008**, *82*, 11084-11095.
64. Dweep, H.; Sticht, C.; Gretz, N. In-silico algorithms for the screening of possible microRNA binding sites and their interactions. *Current genomics* **2013**, *14*, 127-136.
65. Thody, J.; Moulton, V.; Mohorianu, I. PAREameters: a tool for computational inference of plant miRNA–mRNA targeting rules using small RNA and degradome sequencing data. *Nucleic Acids Research* **2020**, *48*, 2258-2270.
66. Pinzón, N.; Li, B.; Martinez, L.; Sergeeva, A.; Presumey, J.; Apparailly, F.; Seitz, H. microRNA target prediction programs predict many false positives. *Genome research* **2017**, *27*, 234-245.
67. Kertesz, M.; Iovino, N.; Unnerstall, U.; Gaul, U.; Segal, E. The role of site accessibility in microRNA target recognition. *Nature genetics* **2007**, *39*, 1278-1284.
68. Golyshev, V.; Pyshnyi, D.; Lomzov, A. Calculation of Energy for RNA/RNA and DNA/RNA Duplex Formation by Molecular Dynamics Simulation. *Molecular Biology* **2021**, *55*, 927-940.
69. Ghoshal, A.; Shankar, R.; Bagchi, S.; Grama, A.; Chaterji, S. MicroRNA target prediction using thermodynamic and sequence curves. *BMC genomics* **2015**, *16*, 1-21.
70. Kaja, E.; Szcześniak, M.W.; Jensen, P.J.; Axtell, M.J.; McNellis, T.; Makałowska, I. Identification of apple miRNAs and their potential role in fire blight resistance. *Tree Genetics & Genomes* **2015**, *11*, 1-11.
71. Liu, X.-X.; Luo, X.-F.; Luo, K.-X.; Liu, Y.-L.; Pan, T.; Li, Z.-Z.; Duns, G.J.; He, F.-L.; Qin, Z.-D. Small RNA sequencing reveals dynamic microRNA expression of important nutrient metabolism during development of Camellia oleifera fruit. *International journal of biological sciences* **2019**, *15*, 416.
72. M Witkos, T.; Koscianska, E.; J Krzyzosiak, W. Practical aspects of microRNA target prediction. *Current molecular medicine* **2011**, *11*, 93-109.